Fingerprinting construction sand supply-networks for traceable sourcing

Zachary T. Sickmann[1,2]*

(* denotes first and corresponding author; zachary.sickmann@utdallas.edu)
[1]*Institute for Geophysics, University of Texas at Austin, Austin, TX, USA*
[2]*Department of Geosciences, University of Texas at Dallas, Dallas, TX, USA (current address)*

Nicholas C. Lammers[3]

[3]*Biophysics Graduate Group, University of California at Berkeley, California 94720*

Aurora Torres[4,5],

[4]*Georges Lemaître Earth and Climate Research Centre, Earth and Life Institute, Université catholique de Louvain, Louvain-la-Neuve, Belgium*
[5]*Center for Systems Integration and Sustainability, Department of Fisheries and Wildlife, Michigan State University, East Lansing, MI, USA*

this is a non-peer reviewed preprint submitted to EarthArXiv

ABSTRACT

Globally increasing demand for construction sand needs to be met with transparent and responsible supply-networks. Currently, there are no scalable methods for tracing construction sand distribution without direct observation. We examined sand "fingerprinting" as a potential tool to trace construction sand supply-networks from "source to sink" in a case study from Texas, USA. Both natural bulk major element and optical petrography fingerprints are preserved through construction sand processing and transport such that sand can be tied back to its original mining source even at the final point of distribution. Additionally, we developed an image analysis model called *sandID* that is ~90% effective at determining the original mining source of sand in the study area. Our results demonstrate that sand fingerprinting, has untapped potential to support traceability and certification schemes and to support monitoring and enforcement in areas where there are concerns about illegal, illicit or simply unknown construction sand sourcing.

INTRODUCTION

Sand is a foundational material to both natural and human systems. From concrete to silicon microchips, the modern world needs more construction aggregates (mainly sand and gravel) than any other solid material resource (1). As demand for sand continues to increase, the impacts of the extraction and use of sand resources on biodiversity and society are increasingly reported and recognized (2, 3, 4). Ensuring that sand resources for urban and infrastructure development are extracted and transported in a socially and environmentally sound manner represents an urgent need (5).

Over the last decade, 'responsible sourcing' and traceability of supply-networks has become a topic of broad interest, as a way to address issues from human health risks in food sources (e.g., sea lettuce [6]; bivalves [7]) to sustainability risks in commodity mineral supply-chains (8) or illegal trade (e.g., to determine the origin of stolen gold [9] or poached ivory [10]). In the mining sector, responsible sourcing has been traditionally applied to the so-called "conflict minerals" (tin, tantalum, tungsten, diamonds, cobalt,

and gold) (11). Despite the scale and importance of the construction sector, for which most sand is extracted (12), the traceability of sand and other construction aggregates is still at an emerging stage (13). This is despite the fact that the development of traceability tools to certify and verify the geographic origin of sand resources, along with strong regulations and monitoring systems, are increasingly encouraged by international organizations to guarantee sustainable outcomes (5). The current paucity of metrics by which to assess the efficacy of any effort to set sustainable sourcing standards or instate traceability in the construction aggregate sector is a hurdle that must be overcome before any such efforts can be broadly successful.

Here, we present a proof-of-concept study that examines the potential of sand provenance analysis or compositional "fingerprinting" in tracing construction sand supply-networks. Compositional fingerprinting methods widely used in sedimentology could provide a way to both monitor and re-construct unknown or poorly defined sand supply-networks, i.e., the connections among sourcing areas, processing and storage sites, and markets (3). Naturally occurring sand inherits a compositional fingerprint from the unique surface geology in the catchment from which it was eroded. Dozens of techniques exist to "fingerprint" sand and tie it back to its source from bulk mineralogy (14) and geochemistry (15) to more sophisticated techniques that build signatures from isotopic compositions of domains within individual sand grains (16). Decades of work exist on the geologic controls on different sand compositions and how to leverage this information to trace sand dispersal pathways in natural sedimentary systems.

Moreover, applications of sand fingerprinting have not been limited to natural systems, with documented success in forensic geology (17, 18, 19) and archaeology (20, 21, 22) in answering questions rooted in understanding the provenance of sand at a crime scene or in an artefacts. However, the potential of these methods for tracing construction sand supply-networks from "source to sink" remains untested. Other than the fact that construction sand is transported via truck, barge or rail car instead of rivers, waves or wind, there is little practical difference in applying sand provenance analysis to commodity supply-networks vs. natural dispersal systems. To test the utility of fingerprinting methods in tracing construction

sand supply-networks, we conducted a first of its kind proof-of-concept study in central and north Texas, USA (Fig. 1).

We aimed to address three research questions crucial to understanding the potential of sand fingerprinting for construction sand traceability and monitoring applications. First: Are natural sand compositional signatures preserved through processing of construction sand? Although post-extraction processing is minimal in some supply-networks, construction sand intended for use in a concrete-type products is often washed and size sorted between extraction from natural deposits and final use (23). Knowing if this processing deleteriously alters sand compositional fingerprints is a crucial first step in considering applying fingerprinting to construction sand supply-networks. Second: Can sand compositional fingerprints trace construction sand supply-networks at a useful spatial scale? Any natural sand will have a definable compositional fingerprint but it is crucial to understand the conditions required to use that fingerprint to trace construction sand supply networks. Third: Can machine learning-aided image analysis be used as a more exportable and inexpensive sand fingerprinting method? One of the potential challenges to the utilization of fingerprinting methods for sand traceability might be the relatively high cost of conventional provenance analysis. When considering all costs from sample preparation through analysis, conventional sand provenance methods range from around $50 to over $1,000 per sample (Fig. 2). While these costs may be reasonable for academic studies, agencies in high-income countries, and large industries, the broad adoption of sand fingerprinting as a scalable monitoring approach in low-income and under-served areas requires low-cost analytical tools.

Proof-of-Concept: Texas Sand Supply-Networks

We collected 41 sand samples across seven sourcing areas of construction sand supply-networks in Texas, USA (Fig. 3). Four of the sampled supply-networks comprise regional distribution of bagged concrete produced in four plants each with its own mine spread out over approximately 900 km across the state. These plants are located in the cities of Amarillo, Abilene, San Antonio and east of the city of

Houston. To sample sand from these four, we procured bagged concrete samples at local hardware stores across the state. Bagged concrete is sold as a dry mixture of sand, gravel and cement that is mixed with water by the end user and is intended for applications that require only a small amount of concrete. As a value-added product, bagged concrete is generally shipped over much wider distribution networks than raw construction sand.

The rest of the samples belong to a series of denser, more complex, supply-networks of sand mines and concrete batch plants across the cities of Austin and San Antonio and their surrounding peri-urban areas (Fig. 3B). To encompass material from these supply-networks, we sampled natural sand from sand mine pits, processed construction sand (washed and size sorted) at the mining site, and sand from sand stockpiles at concrete batch plants. Concrete batch plants mix large volumes of sand, gravel and cement on site to generate batches of wet concrete that are then transported to local construction sites. Mines in this region process sand in classifiers that largely work on hydrodynamic and specific gravity sorting (Sims and Brown, 1998). These classifiers take raw natural pit sand and sort it into size ranges that match the desired engineering specifications that the mining site has set for various construction sand products like concrete or masonry sand.

The sampled suppliers source sand from seven different geologic units (24): 1) Holocene-age and 2) Pleistocene-age terraces of the upper Colorado River in and around the city of Austin, 3) modern sand from the Llano River near the town of Llano, 4) Pleistocene terraces of the lower Colorado River, 5) Paleogene-age shallow marine sand deposits preserved in an arcuate outcrop belt across central Texas (Fig. 3); tapped in the mines in our study in an area just south of San Antonio, 6) Pleistocene sands near Abilene and 7) Pliocene to Miocene-age sand deposits near Amarillo (Fig. 3). For the purposes of our study, these seven sand sources offer useful range in determining the resolution at which supply-networks can be distinguished in the four sources (Llano River, Holocene up. Colorado, Pleistocene up. Colorado and Pleistocene low. Colorado River) within the same natural sediment dispersal system (Fig. 3) and the other three (San Antonio, Abilene and Amarillo), which are entirely unique and unrelated geologically.

RESULTS and DISCUSSION

Preservation of Fingerprints through Construction Sand Processing

To test if natural sand compositional signatures are preserved through construction sand processing, we sampled raw pit sand and processed sand products sourced from four mining areas: 1) San Antonio, 2) Holocene upper Colorado River terraces, 3) Pleistocene upper Colorado River terraces and 4) the Llano River (Fig. 4AB). To encompass pre and post processing, we sampled both raw pit sand and processed sand at each site (excluding the Llano River mine, where we only sampled raw river sand from the mining area) and sand from stockpiles at concrete batch plants from known sources. For batch plant samples, we confirmed with the mine-site manager where on-site sand came from, ensuring that we were comparing sand samples from the same original set of mines across the study area. We were only able to sample sand from the final product in bagged-concrete distribution networks. Therefore, those samples are not included in this section. We found that by bulk major element geochemistry and framework mineralogy, natural compositional sand fingerprints are preserved through processing such that compositional fingerprint variability between mining areas is much greater than compositional variability within sample sets from each area (Fig. 4CD). However, bulk trace element geochemistry shows that there is some density fractionation during processing suggesting that care should be taken in using compositional fingerprints that rely on heavy minerals (Fig. 5).

By bulk major element geochemical signatures ($[Al_2O_3 + K_2O]$ vs. SiO_2; Fig. 4C) and framework mineral petrography (Fig. 4D), all four mining areas are clearly distinguishable with the silica rich San Antonio sand samples particularly distinct from sand in the Llano - upper Colorado River areas (Fig. 4). The relative similarity between Llano River and Holocene and Pleistocene upper Colorado River terraces sands is unsurprising considering the fact they are part of the same regional natural sand dispersal system. However, particularly in major element geochemistry, they all plot in distinct, non-overlapping fields (Fig. 4C). Interestingly, sand from Pleistocene upper Colorado River terraces is distinct from sand from Holocene

upper Colorado River terraces across all sampled stages in the local construction sand supply-network (Fig. 4CD). Spatially, the closest of these mining sites are separated by less than 5 km (Fig. 4B). Natural variation in compositional sand fingerprints between Pleistocene and Holocene Colorado River terraces is further supported by previous studies focused on the natural sand dispersal system and is attributed to variations in climate and weathering regimes since the last glacial maximum (25).

To further assess potential processing fractionation, we also sampled and analyzed masonry sand from two mines in the upper Colorado River mining area; uCRm1 in Holocene terraces and uCRm4 in Pleistocene terraces (Fig. 4B). Masonry sand represents the most heavily processed product that these mines produce as it needs to be consistently fine, well-sorted and clean; generally much finer and better sorted than the bulk sand grain size in area mining pits (Fig. 5A). Masonry sand results are only considered in this section on examining fractionation and are not compared to concrete sands in any other section. To look for potential compositional fraction by mineral density, we compared the Zirconium (Zr) concentration, bulk Rare Earth Element (REE) signatures, and major element geochemical signatures of each sample (Fig. 5ABC). The granitic rocks of central Texas in the Colorado River catchment are known to be particularly fertile with respect to detrital zircons (Dickinson, 2008). With a chemical formula of $ZrSiO_4$, zircon is the primary mineral host for Zr in most sands (26) and with a specific gravity of 3.9 – 4.7, the concentration of the mineral is a useful proxy for heavy mineral fractionation (27, 28). Masonry sand from both uCRm1 and uCRm4 is notably elevated in Zr concentration even as compared to natural pit sand of a similar grain size (uCRm1 fine raw pit sand vs. masonry sand; Fig. 5), suggesting that mine-site processing is enacting some heavy mineral fractionation. This is also perhaps suggested with the enrichment of light REEs (La – Gd) in masonry sand particularly from the uCRm1 site (Fig. 5).

However, the bulk major element composition of masonry sand from uCRm1 is similar to fine raw pit sand from the same site with both relatively depleted in Al_2O_3 and K_2O as compared to coarser pit sand and concrete sand. Masonry sand at uCRm4 is also relatively depleted in Al_2O_3 and K_2O as compared to raw pit sand and concrete sand from this mine (finer pit sand was unavailable from this site). This depletion

187 in Al_2O_3 and K_2O likely reflects a natural difference in the composition of sand at each site by grain size, a
188 common feature of natural sands (27).

189 Cumulatively, results from these four supply-networks suggest that any fractionation that does
190 occur when processing construction sand is unlikely to affect bulk major element and other framework
191 mineralogy fingerprints like optical petrography QFL. However, care must be taken that the compositional
192 fingerprint used to represent the raw natural source sand is of the correct grain size to match the grain size
193 of the construction sand product in question and mineral density fractionation needs to be considered when
194 using trace element geochemistry or methods the rely on heavier minerals like detrital zircon.

195 **Defining Supply-Networks with Conventional Fingerprinting techniques**

196 After determining that intra-source area variance in compositional fingerprints was much less than
197 inter-source area variance, we set out to identify the resolution with which construction sand supply-
198 networks can be reconstructed by conventional provenance methods and the specific conditions that must
199 be met to do so. For this, we added compositional sand fingerprints from regional bagged concrete samples
200 to the central Texas networks described above. As with local mine-to-batch plant networks in central Texas,
201 sand from each bagged concrete plant produces a distinct compositional fingerprint by bulk major element
202 geochemistry and QFL petrography and each of the four is entirely distinct from the central Texas networks
203 (Fig. 6A). Even sand from the San Antonio bagged-concrete plant is distinguishable from San Antonio-
204 derived sand mine and concrete batch plant sand; a finding we encountered while iterating the image
205 analysis methods described below and then confirmed by the bulk major element geochemistry. This
206 distinction derives not from any natural differences in sand composition as all San Antonio sand is mined
207 from the same silica-rich Paleogene sand deposit (>95 wt% SiO_2) but instead from the fact that the San
208 Antonio bagged-concrete plant mixes natural sand with crushed limestone as the coarse aggregate to
209 produce their final product. Particles of crushed limestone remained in the sand-sized fraction of material
210 we analyzed for this study resulting in San Antonio-derived bagged concrete having systematically higher

bulk Calcium content (wt% CaO; Fig. 6A). This plant therefore introduces useful artificial compositional variability not present in the natural sand deposit that can be used in fingerprinting.

The fact that all eight sourcing areas sampled for this study are distinct and distinguishable across extraction, processing and transport is an encouraging sign for using sand fingerprinting in tracing supply-networks. These results also illustrate the specific conditions required to employ these techniques. Where natural compositional variability exists between two sand sources (by any provenance method), as here in Texas, that variability is likely to be preserved from "source to sink" in a construction sand supply-network. Additionally, if the processing phase adds compositional variability, by mixing sands from multiple sources (e.g., naturally occurring sands and crushed rock), as in the example of the San Antonio bagged-concrete plant, fingerprinting will also be effective. However, if no compositional variability exists, fingerprinting will be ineffective. As an example of this counterpoint, we cannot distinguish sand, by any fingerprinting method employed in this study, sourced from the uCRm1, 2 nor 3 sites (uCRm: upper Colorado River mine) which all mine from Holocene upper Colorado River (Fig. 4BCD). By coincidence, the concrete batch plants we sampled for this study that sourced sand from the upper Colorado River mining area all sourced from uCRm4 specifically.

Had any of those plants sourced from uCRm1, 2 or 3, we would not have been able to independently distinguish which specifically it came from with compositional fingerprinting. Similarly, the Paleogene silica-rich sand deposits that are mined south of San Antonio extend in an arcuate outcrop belt across the entire central Texas study area (Fig. 4A). If there were mines extracting from those deposits in the Austin area, it is unlikely that we would have been able to distinguish that sand from sand mined south of San Antonio.

The efficacy of compositional fingerprinting therefore depends on both natural (or artificial) variability in sand composition and the internal complexity of the sand-sourcing regime of the supply-network in question. This is to say that there must be heterogeneity in the natural fingerprints of the sourcing

areas and the networks must be sufficiently diverse to leverage that heterogeneity into answering an impactful question on sand sourcing. If both of these requirements are not met, sand fingerprinting is unlikely to be effective.

How sand fingerprinting might be used at the final site of consumption depends on the use of the sand. If the sand is used in an unconsolidated state as landfill, sand fingerprinting as described here can be employed. If it is set with cement in a concrete product, optical petrography is likely still viable as a sample can be cut and polished into a thin section in the same way as natural sandstone. However, applying bulk geochemical methods may not be viable as the cement will alter the elemental signature. Further work is needed to unravel how best to fingerprint sand from set-concrete.

Cost effective sand fingerprinting with machine learning image analysis

Although conventional provenance analysis methods clearly have potential in fingerprinting construction sand supply-networks from "source to sink," the analytical facilities within which to conduct conventional provenance analysis are not ubiquitous globally nor is analytical funding. For our case study in Texas, we used relatively inexpensive methods of optical petrography and bulk geochemistry that allowed us to collect, process, and analyze our 41 sand samples for a cost of ca. $20,000. This is a relatively modest budget for a large-scale conventional provenance study but may be prohibitive in some places. Fortunately, in addition to geochemical and petrographic signatures that can be expensive to unravel, natural sand from different deposits often has systematic differences in grain size, shape and color all owing to natural mineralogy and local sedimentary processes. We reasoned that these same features could be leveraged by an algorithm to predict provenance using images of sand samples.

To test the viability of such an approach, we developed an image classification pipeline, *sandID*, which uses transfer learning (29) to train a deep convolutional neural network to predict sample provenance using photos of sand captured with an iPhone. The *sandID* model is, on average, 86% effective at

identifying the original source of mined concrete sand in our Texas study area (Fig. 7). A significant fraction of prediction error derives from mix-ups between samples taken from the Holocene and Pleistocene river terraces on the upper Colorado River which are only subtly different compositionally by conventional methods as described above. Combining these categories yields an average accuracy of 91% in provenance prediction.

We found that the relative placement of our samples within the t-Distributed Stochastic Neighbor Embedding (t-SNE) plots, which describe what *sandID* "sees" as differences between samples, recapitulates natural relationships between sand sources and relative natural compositional variability. The Llano River and Colorado River samples cluster closely together (Fig. 7), reflecting that these sources belong to the same sediment dispersal system. Sand from different bagged concrete plants plot in distinct clusters relatively far apart (Fig. 7). Our results therefore suggest that regionally keyed machine learning models may be useful tools for sand fingerprinting in any area with sufficient compositional differences. The *sandID* tool requires only a personal laptop to run and, once trained, takes only seconds to classify new sand samples at no additional cost outside of the labor required to collect and photograph the samples. Thus, we conclude that this method hold promise as a scalable approach for fingerprinting sand provenance that should be readily exportable to settings lacking access to specialized and expensive methods of provenance analysis.

Beyond its utility for predicting sand provenance, *sandID* can also function as a tool for uncovering salient heterogeneity within sand sources that may not be apparent in initial conventional analysis. We originally trained *sandID* with seven defined source populations: 1) Amarillo, 2) Abilene, 3) Llano River, 4) upper Colorado River Hol., 5) upper Colorado River Pleis., 6) lower Colorado River and 7) San Antonio under the assumption that the model would not be able to distinguish San Antonio bagged concrete sand from mine and concrete batch plant sand. Differences between the two sands which are >95 wt% SiO_2 are subtle at best in the conventional compositional fingerprints we initially plotted (Fig. 6). However, even when trained on a lumped San Antonio source, *sandID* suggested there were multiple San Antonio

provenance families, with the two groups on the left-hand side of Fig. 7A reflecting samples from San Antonio mines and batch plants ("SA m&bp") and the group on the right-hand side reflecting San Antonio bagged concrete.

We then revisited the conventional geochemistry data and realized that bagged concrete sand has elevated CaO content owing to the fact the plant adds crushed limestone to the otherwise silica-rich sand (Fig. 7); a real and useful artificial difference in source fingerprints. Conversely, we find that the presence of two distinct clusters within the mine and batch plant population (SA m&p; Fig. 7B) reflects differences in grain size. When we sieved all samples at 500 microns and reimaged a medium sand and finer image training set for all samples, these sub-populations collapse into one cluster while the distinction from bagged concrete remains (Fig. 7). These results emphasize the need for care when interpreting model outputs and the utility in analyzing iteratively and ideally having at least some conventional compositional fingerprint data to validate results.

IMPLICATIONS AND NEXT STEPS

Our results conclude that sand fingerprinting, whether with conventional provenance methods or novel image analysis approaches, has an untapped potential as a monitoring tool to support traceability systems (e.g., certification schemes) and to support monitoring and enforcement in areas where there are concerns about illegal, illicit or simply unknown construction sand sourcing. A few particular facts about the success of our case study in Texas can be extrapolated to discuss potential for success in other places globally. First, Texas is not particularly geologically complex. The abundant leverage in compositional fingerprinting and image analysis in these passive margin sand deposits bodes well for regions with more complex surface geology in adjacent sand dispersal system catchments like South and Southeast Asia. Countries like Bangladesh, Myanmar, Laos and Malaysia show greater than 20% average annual growth in aggregate consumption of the last 20 years (Fig. 8), are known areas of sand mining conflict (30, 31) with opaque sand sourcing issues and are among the most geologically complex areas in the world. As an

example of potential fingerprinting leverage in this region we highlight summaries of known compositional variability in sand across Bangladesh and Myanmar from previously published work in Fig. 8.

In Bangladesh, sand from the Ganges, Brahmaputra and Syhlet drainages are robustly distinguishable by their Strontium concentration and isotopic signatures (Fig. 8; 32). In cities like Khulna and Dhaka, concrete construction projects source sand from one or a mix of these three sources (33, 34), often without knowing from which it came (35). While literature on the sources of construction sand for specific localities in Myanmar is less well-developed than for Bangladesh, it is clear that both outer coast beaches and the Irrawaddy River are both important sources of sand for the domestic construction industry and for export abroad (36). The upper and lower Irrawaddy and coastal sands in Myanmar are all robustly distinguishable based on both framework mineralogy and bulk geochemistry (37; Fig. 8). The composition of sands across Myanmar is even more variable than that identified in Texas construction sand sources in our case study. Myanmar may therefore not only be a prime candidate for conventional provenance fingerprinting but also image analysis. Such compositional leverage is also likely present in other areas in South and Southeast Asia. There is simply currently not enough published data in most other countries to highlight the potential here.

A second finding from Texas that bodes well for broader exportation of sand fingerprinting for effective monitoring and certification is the fact that natural compositional variability between Pleistocene and Holocene river sand terraces from closely spaced mines in the same river valley are preserved through the supply-network. Natural climate cycles over ten to hundred thousand year time scales are known to shift sand composition due to both drainage reorganization and changing weathering regime in many places globally (e.g. 38, 39, 40). Many sand extraction environmental sustainability issues boil down to mining from active sand dispersal systems vs. older sand deposits (e.g. modern river sand bars vs. older river sand terraces). Consequently, the regulations of many regions across the world forbid or limit the extraction of sand from active river channels for the construction industry (3). If, as in the upper Colorado River in Texas, young or modern sand in a given river of concern is distinguishable from older river terraces, it may be

possible to develop a location-specific certification scheme that can flag unauthorized extraction from the modern river vs. extraction from older terraces.

Broadly speaking, fingerprinting will likely be useful in any traceability strategy that includes certification and verification of the geographic origin of sand resources and could be used to ensure the correct performance of responsible sourcing schemes. There are a growing number of management frameworks designed specifically to assess, audit and certify supply chains for construction materials (41). By providing a method to independently confirm the geographic origin of samples, sand fingerprinting could identify illegal extraction and fraudulent trade practices. Responsible sourcing applications of these methods are particularly interesting in regions and countries with existing regulatory concerns and active illicit supply-networks (42) and in places with limited local supply that rely heavily on imports such as Singapore (5) or Hong-Kong (70%; 43). The full spectrum of specific applications of fingerprinting construction sand supply-networks is likely broader than we have currently described. Having demonstrated that this approach is effective in principle and provided a new tool in *sandID* to make it more broadly accessible and exportable, more work is needed to continue to expand applications of sand fingerprinting to making human sand supply-networks more transparent, equitable and sustainable.

MATERIALS and METHODS

Sample Collection and Processing

We collected all 41 samples used in this study from July through September of 2021. Sand samples from sand mines (n = 15) were directly collected with cooperation from mine-site personnel from 6 different mines. We would arrive at the mine and be driven to the active mining front in the sand pit by the mine-site manager. We collected one or two raw pit sand samples from the area of the raw natural sand deposit being mined that day. Processed sand samples were collected directly in the processing area from the active stockpile below the outflow of the mine site's aggregate classifying machinery. At 5 different concrete

355 batch plants, we collected 7 samples from sand stockpiles (two batch plants had sand from two different
356 mining sources in their stockpiles) and confirmed the original source of the sand from the plant manager.
357 Bagged concrete samples were purchased at local hardware stores in the sampling localities (n = 19).

358 Bagged concrete comes as pre-mixed cement, sand and gravel. We washed sand and gravel out of
359 the cement-aggregate mixture by hand in a five-gallon bucket. We dumped approximate 3-4 kg of the
360 cement-aggregate mixture into the bucket and filled the bucket with water while mixing until the bucket
361 was nearly full. We then let the aggregates settle out of suspension and the cement-laden water was decanted
362 off. We repeated this process until the water was clear and then dried the sample. For all raw pit mine sand
363 samples, we washed out any top soil or mud present in the sample using a similar decanting method. All
364 samples were sieved at 2 mm. This sample processing was all done before samples were sub-sampled for
365 any further analysis.

366 **Grain Size Analysis**

367 We conducted grain size analysis for sand samples from the upper Colorado River mines (Fig. 4)
368 from which we collected a full suite of raw, concrete and masonry sand using a 2-meter settling column.
369 Sand is poured into the top of the column tripping a timer and the rate of mass accumulation is measured at
370 a scale at the bottom of the column as grains settle through the water in the column. Measurement continues
371 for 10 minutes after which time a simple program calculates the grain size distribution of the sample at
372 quarter-Phi resolution assuming Stokes Law settling velocities:

373

374 $$v = \frac{2}{9}\frac{(\rho_p - \rho_f)}{\mu} g R^2$$

375 Where: v = settling velocity, ρ_p = particle density (assumed to be 2.65 g/cm^3 in this setup), ρ_f =
376 fluid density, μ = fluid viscosity, g = acceleration due to gravity, and R = particle radius.

377 **Conventional Compositional Fingerprinting**

We analyzed all sand samples with optical petrography and bulk major and trace element geochemistry. Optical petrography consisted of point counting grain-mount thin sections using the Gazzi-Dickinson method in which every sand-sized mineral (>62.5 μ) is counted individually. This method is designed to reduce grain size bias and produces a result that reflects the bulk framework mineralogy of the surface geology in the catchment from which the sand eroded. We counted 400 points per thin section. Full optical petrography results are available in supplemental material. Bulk sand geochemical analyses were conducted at the Washington State University (WSU) Peter Hooper GeoAnalytical Lab. Bulk major and trace element geochemistry was determined via X-ray fluorescence analysis (XRF) and inductively coupled plasma mass spectrometry (ICPMS). XRF analyses were conducted on a Thermo-ARL automated X-ray fluorescence spectrometer. XRF sample material was analyzed in a Li-tetraborate fused bead. ICPMS analyses were conducted on an Agilent inductively coupled plasma mass spectrometer. Full data tables for all geochemical results are further detailed references for geochemical methods can be found in supplemental material.

We display bulk major element results here as ($Al_2O_3 + K_2O$) vs. SiO_2 as this is a particularly useful discriminator in our study area, which largely derives from natural differences in plagioclase feldspar, potassium feldspar (K-spar) and quartz content across samples. Aluminum and Potassium are hosted preferentially in the feldspars while Silica derives preferentially from quartz. Combining Aluminum and Potassium accentuates the presence of K-spar in Colorado River catchment sands eroded in part from central Texas granites.

Machine Learning Image-Analysis: *sandID*

As described above, we generated image analysis results from sample material sieved at 2 mm and at 500 microns to look for grain size bias in results. The sub-500 micron fraction was only analyzed via image analysis. The first step in our image analysis process was generating a dataset of sand images that could then be used to train the image classification model. To generate a training dataset containing images

of sand samples, we placed material from each sample in a 5 cm diameter PVC pipe cap, and took a photograph directly overhead from approximately 15 cm away using an iPhone 12. The phone's camera was set to all standard, default, settings. Through this process, we produced 76 distinct images of our sand samples (two different images of each sample [n = 38]; excluding the 3 masonry and fine put sand samples). Due to the random nature of sand distribution within each large-scale sample image, it was possible to subdivide each for the 76 images computationally into smaller 176 x 176 pixel image squares, each of which could serve as a separate training sample. This produced a dataset containing 1,690 sample images of sand, with at least 150 sample images per supply network category. This process was repeated for the sub-500 micron image set as well.

For our image classification model, we took GoogLeNet as our starting point, which is a deep convolutional neural network with 22 layers that was originally trained to classify 1000 distinct everyday objects (e.g., keyboard, mouse, pencil). We retrained the model to predict the provenance of different sand samples from our case study sample set using105 images from each source. We used standard back-propagation methods for training. We held out 45 images per source and used these as a validation set to periodically gauge model accuracy over the course of training. All scripts for image sample generation, and for the analysis and visualization of provenance predictions were implemented in Matlab 2020a, and are available on GitHub at https://github.com/nlammers371/sandID.git as are the 76, full-size, sample images that formed the basis of the training set.

REFERENCES CITED

1. OECD, *Global Material Resources Outlook to 2060: Economic Drivers and Environmental Consequences* (Organisation for Economic Co-operation and Development, Paris, 2019; https://www.oecd-ilibrary.org/environment/global-material-resources-outlook-to-2060_9789264307452-en).
2. M. Bendixen, L. L. Iversen, J. Best, D. M. Franks, C. R. Hackney, E. M. Latrubesse, L. S. Tusting, Sand, gravel, and UN Sustainable Development Goals: Conflicts, synergies, and pathways forward. *One Earth*. **4**, 1095–1111 (2021).
3. A. Torres, M. U. Simoni, J. K. Keiding, D. B. Müller, S. O. S. E. zu Ermgassen, J. Liu, J. A. G. Jaeger, M. Winter, E. F. Lambin, Sustainability of the global sand system in the Anthropocene. *One Earth*. **4**, 639–650 (2021).

4. A. Torres, S. O. S. E. zu Ermgassen, F. Ferri-Yanez, L. M. Navarro, I. M. D. Rosa, F. Z. Teixeira, C. Wittkopp, J. Liu, "Unearthing the global impact of mining construction minerals on biodiversity" (preprint, Ecology, 2022), , doi:10.1101/2022.03.23.485272.
5. U. N. E. P., *Sand and Sustainability: 10 Strategic Recommendations to Avert a Crisis* (2022; https://wedocs.unep.org/xmlui/handle/20.500.11822/38362).
6. R. Mamede, F. Ricardo, M. H. Abreu, E. F. da Silva, C. Patinha, R. Calado, Spatial variability of elemental fingerprints of sea lettuce (Ulva spp.) and its potential use to trace geographic origin. *Algal Research*. **59**, 102451 (2021).
7. R. Mamede, A. Santos, S. Díaz, E. Ferreira da Silva, C. Patinha, R. Calado, F. Ricardo, Elemental fingerprints of bivalve shells (Ruditapes decussatus and R. philippinarum) as natural tags to confirm their geographic origin and expose fraudulent trade practices. *Food Control*. **135**, 108785 (2022).
8. F. Melcher, M.A. Sitnikova, T. Graupner, N. Martin, T. Oberthür, F. Henjes-Kunst, E. Gäbler, A. Gerdes, H. Brätz, D.W. Davis, S. Dewaele, Fingerprinting of conflict minerals: columbite-tantalite ("coltan") ores. *Society for Geology Applied to Mineral Deposits News,* **23**, (2008)
9. R. J. Watling, C. J. Scadding, C. D. May, Chemical fingerprinting of gold using laser ablation–inductively coupled plasma–mass spectrometry (LA-ICP-MS). *Journal of the Royal Society of Western Australia*, 10 (2014).
10. S. K. Wasser, C. Mailand, R. Booth, B. Mutayoba, E. Kisamo, B. Clark, M. Stephens, Using DNA to track the origin of the largest ivory seizure since the 1989 trade ban. *Proc. Natl. Acad. Sci. U.S.A.* **104**, 4228–4233 (2007).
11. S. van den Brink, R. Kleijn, A. Tukker, J. Huisman, Approaches to responsible sourcing in mineral supply chains. *Resources, Conservation and Recycling*. **145**, 389–398 (2019).
12. A. Miatto, H. Schandl, T. Fishman, H. Tanikawa, Global Patterns and Trends for Non-Metallic Minerals used for Construction. *Journal of Industrial Ecology*. **21**, 924–937 (2017).
13. J. Glass, N. Achour, T. Parry, I. Nicholson, Engaging small firms in sustainable supply chains: responsible sourcing practices in the UK construction industry, *International Journal of Agile Systems and Management*, **5**, (2012)
14. W. R. Dickinson, Relations of andesites, granites, and derivative sandstones to arc-Trench tectonics. *Reviews of Geophysics*. **8**, 813–860 (1970).
15. S. M. McLennan, S. Hemming, D. K. McDaniel, G. N. Hanson, Geochemical approaches to sedimentation, provenance, and tectonics (1993), doi:10.1130/SPE284-p21.
16. G. Gehrels, Detrital Zircon U-Pb Geochronology Applied to Tectonics. *Annual Review of Earth and Planetary Sciences*. **42**, 127–149 (2014).
17. G. Lombardi, The contribution of forensic geology and other trace evidence analysis to the investigation of the killing of Italian Prime Minister Aldo Moro. *J Forensic Sci*. **44**, 634–642 (1999).
18. K. M. Pitts, R. M. Clarke, The forensic discrimination of quartz sands from the Swan Coastal Plain, Western Australia. *Forensic Science International: Reports*. **2**, 100130 (2020).
19. L. J. Donnelly, D. Pirrie, M. Harrison, A. Ruffell, L. A. Dawson, *A Guide to Forensic Geology* (Geological Society of London, 2021).
20. W. R. Dickinson, "Temper Sands in Prehistoric Oceanian Pottery: Geotectonics, Sedimentology, Petrography, Provenance" in *Temper Sands in Prehistoric Oceanian Pottery: Geotectonics, Sedimentology, Petrography, Provenance* (Geological Society of America, 2006; https://pubs.geoscienceworld.org/books/book/553/chapter/3802353).
21. R. De Luca, D. Miriello, A. Pecci, S. Domínguez-Bella, D. Bernal-Casasola, D. Cottica, A. Bloise, G. M. Crisci, Archaeometric Study of Mortars from the Garum Shop at Pompeii, Campania, Italy. *Geoarchaeology*. **30**, 330–351 (2015).
22. P. N. Owens, W. H. Blake, L. Gaspar, D. Gateuille, A. J. Koiter, D. A. Lobb, E. L. Petticrew, D. G. Reiffarth, H. G. Smith, J. C. Woodward, Fingerprinting and tracing the sources of soils and sediments: Earth and ocean science, geoarchaeological, forensic, and human health applications. *Earth-Science Reviews*. **162**, 1–23 (2016).
23. I. Sims, B. Brown, "Concrete Aggregates" in *Lea's Chemistry of Cement and Concrete* (2003), pp. 907–1015.
24. Bureau of Economic Geology (BEG), Geologic Atlas of Texas, (2014)
25. E. Gutierrez, S. F Daniel, J., Covault, "PLEISTOCENE TO HOLOCENE CLIMATE-MODULATED CHANGES IN FLUVIAL GEOMORPHOLOGY AND DETRITAL ZIRCON PROVENANCE IN

CENTRAL TEXAS RIVERS" in (GSA Abstracts, 2020; https://gsa.confex.com/gsa/2020AM/webprogram/Paper355094.html).

26. W. R. Dickinson, Impact of differential zircon fertility of granitoid basement rocks in North America on age populations of detrital zircons and implications for granite petrogenesis. *Earth and Planetary Science Letters*. **275**, 80–92 (2008).
27. E. Garzanti, S. Andò, G. Vezzoli, Grain-size dependence of sediment composition and environmental bias in provenance studies. *Earth and Planetary Science Letters*. **277**, 422–432 (2009).
28. M. D. Cantine, J. B. Setera, J. A. Vantongeren, C. Mwinde, K. D. Bergmann, Grain size and transport biases in an Ediacaran detrital zircon record. *Journal of Sedimentary Research*. **91**, 913–928 (2021).
29. L. Y. Pratt, "Discriminability-Based Transfer between Neural Networks" in *Advances in Neural Information Processing Systems* (Morgan-Kaufmann, 1992; https://papers.nips.cc/paper/1992/hash/67e103b0761e60683e83c559be18d40c-Abstract.html), vol. 5.
30. S. Khan, A. Sugie, Sand Mining and Its Social Impacts on Local Society in Rural Bangladesh: A Case Study of a Village in Tangail District, 11 (2015).
31. M. Marschke, J.-F. Rousseau, Sand ecologies, livelihoods and governance in Asia: A systematic scoping review. *Resources Policy*. **77**, 102671 (2022).
32. S. L. Goodbred Jr., P. M. Paolo, M. S. Ullah, R. D. Pate, S. R. Khan, S. A. Kuehl, S. K. Singh, W. Rahaman, Piecing together the Ganges-Brahmaputra-Meghna River delta: Use of sediment provenance to reconstruct the history and interaction of multiple fluvial systems during Holocene delta evolution. *GSA Bulletin*. **126**, 1495–1510 (2014).
33. S. Roy, M. Alam, M. Begum, B. Alam, Radioactivity in building materials used in and around Dhaka City. *Radiation protection dosimetry*. **114**, 527–32 (2005).
34. H. Kabir, I. Hoque, T. Rahman, Engineering Properties and Cost Comparison among Sylhet sand, Khustia Sand and Local Sand in the Context of Foundation, 14 (2018).
35. A. Alam, Z. Habib, R. Sheikh, A. Hasan, A Study on the Quality Control of Concrete Production in Dhaka City. *IOSR Journal of Mechanical and Civil Engineering*. **13**, 11 (2016).
36. B. Kadoe, Exploring Sand-Mining in Yangon, Myanmar: Status, Regulations and Impacts, 41 (2018).
37. E. Garzanti, J.-G. Wang, G. Vezzoli, M. Limonta, Tracing provenance and sediment fluxes in the Irrawaddy River basin (Myanmar). *Chemical Geology*. **440**, 73–90 (2016).
38. S. Lugli, S. Dori, D. Fontana, Alluvial sand composition as a tool to unravel late Quaternary sedimentation of the Modena Plain, northern Italy. *Special Paper of the Geological Society of America*. **420**, 57–72 (2007).
39. A. Alizai, P. D. Clift, L. Giosan, S. VanLaningham, R. Hinton, A. R. Tabrez, M. Danish, Pb isotopic variability in the modern-Pleistocene Indus River system measured by ion microprobe in detrital K-feldspar grains. *Geochimica et Cosmochimica Acta*. **75**, 4771–4795 (2011).
40. D. Tentori, K. M. Marsaglia, S. Milli, Sand Compositional Changes As A Support For Sequence-Stratigraphic Interpretation: The Middle Upper Pleistocene To Holocene Deposits of the Roman Basin (Rome, Italy). *Journal of Sedimentary Research*. **86**, 1208–1227 (2016).
41. Responsible sourcing of construction materials BES 6001 - BRE Group (2018), (available at https://bregroup.com/services/standards/responsible-sourcing/).
42. N. Magliocca, A. Torres, J. Margulies, K. McSweeney, I. Arroyo-Quiroz, N. Carter, K. Curtin, T. Easter, M. Gore, A. Hübschle, F. Massé, A. Rege, E. Tellman, Comparative Analysis of Illicit Supply Network Structure and Operations: Cocaine, Wildlife, and Sand. *Journal of Illicit Economies and Development*. **3**, 50–73 (2021).
43. V. J. L. Gan, J. C. P. Cheng, I. M. C. Lo, Integrating life cycle assessment and multi-objective optimization for economical and environmentally sustainable supply of aggregate. *Journal of Cleaner Production*. **113**, 76–85 (2016).
44. UN-IRP. (2018). Global Material Flows Database. from UN International Resources Panel http://www.resourcepanel.org/global-material-flows-database.
45. USGS Minerals Yearbooks: https://www.usgs.gov/centers/nmic/cement-statistics-and-information

ACKNOWLEDGEMENTS

This work was funded by a University of Texas Institute for Geophysics "Blue Sky" grant awarded to the authors. A.T. received funding from the European Union's Horizon 2020 research and innovation programme under the Marie Sklodowska-Curie grant agreement No 846474. We thank Martin Marietta, Texas Materials, Capitol Aggregates and Tex-Mix Concrete for their help and cooperation in sampling sand mines and concrete batch plants. Z.T.S. conceived of and executed the case study and was the primary author of the manuscript. N.C.L., designed and executed the machine learning image analysis model *sandID* and helped author the manuscript. A.T. helped defined the broader impacts of sand fingerprinting on certification schemes and sand sourcing issues and helped author the manuscript. The authors declare that they have no competing interests. All data needed to evaluate the conclusions of the paper are present in the paper and/or the Supplemental Materials. Code for *sandID* is available at https://github.com/nlammers371/sandID.git.

559 **FIGURES**

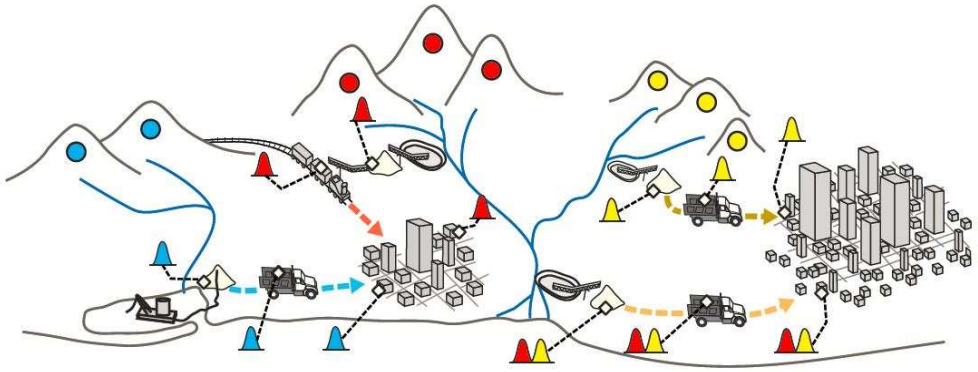

560

561 **Figure 1.** Conceptual schematic for natural sand compositional "fingerprints" carrying through
562 construction sand supply-networks. Natural sand composition is inherited from colour-coded source regions
563 (indicated in circles) and carried through extraction, transport, and use as a discernible schematic signal.
564 The signal can include the mixing of fingerprints from different sources as shown in the lower right.

565

566

567

568

569

570

571

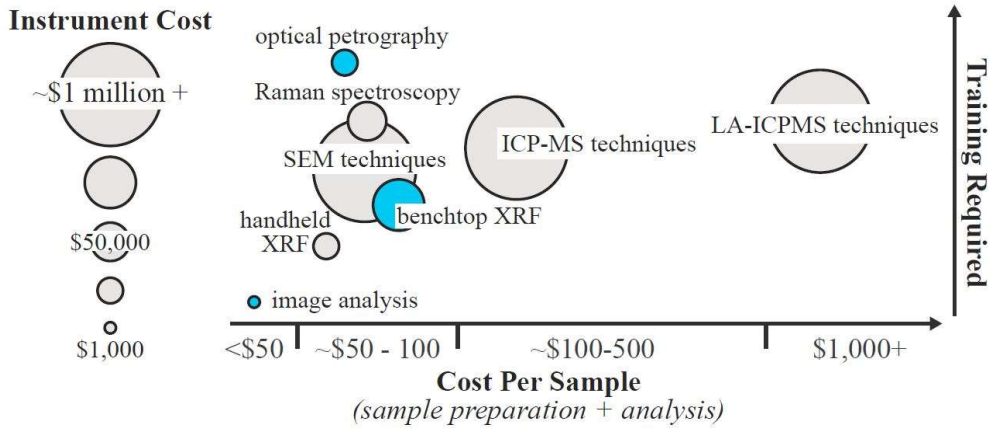

572

573 **Figure 2.** Generalized overview of the training and cost required for various sand provenance or
574 "fingerprinting" methods and the approximate cost of instrumentation required for each type of analysis.
575 Methods employed in this study are highlighted in blue.

576

577

578

579

580

581

582

583

584

585

586

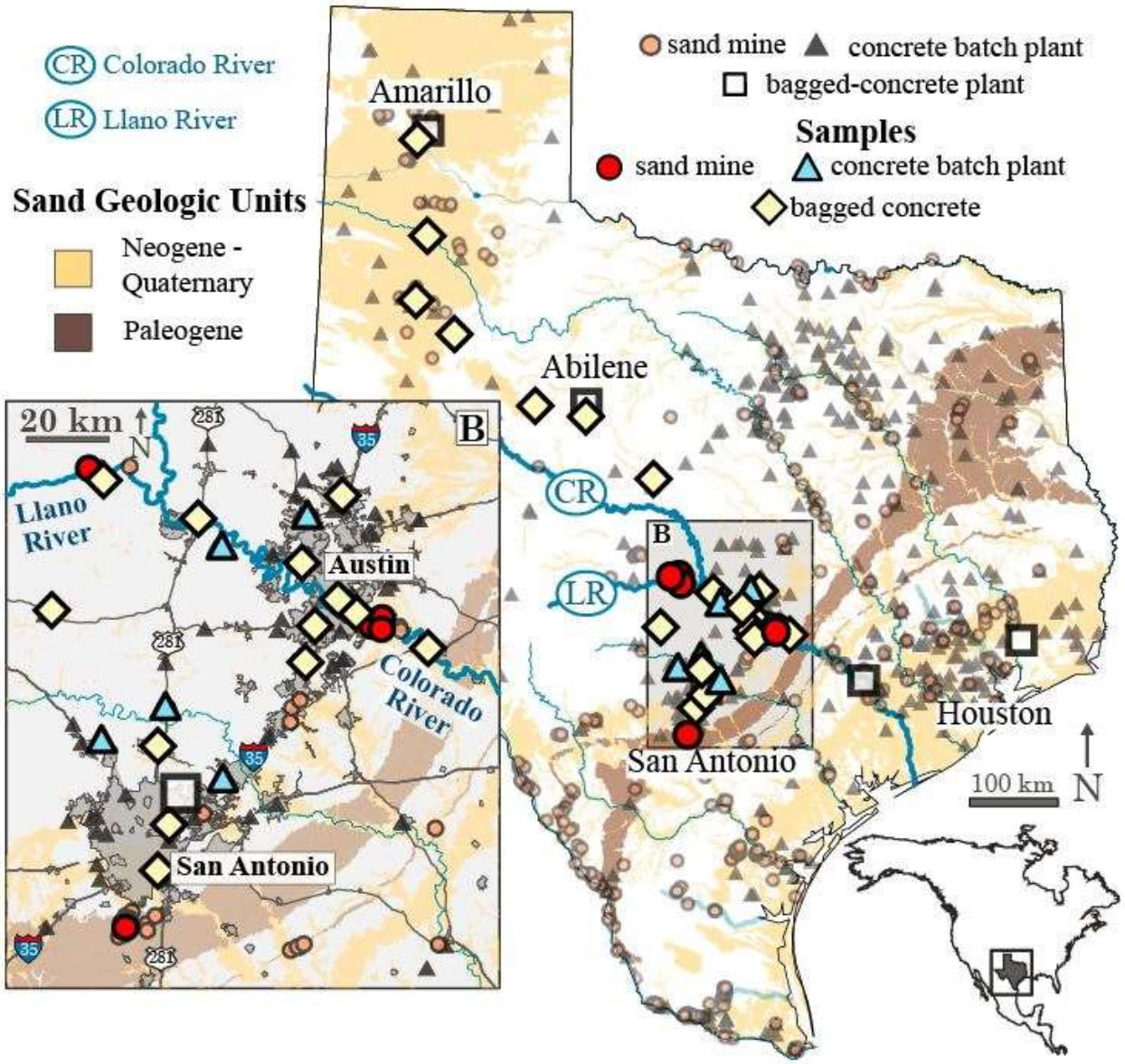

Figure 3. Overview of natural sand deposits (24) and the geography of the construction sand industry in Texas, USA, including sample locations for this study mostly in the San Antonio –Austin area (Panel B) to use compositional fingerprinting over local scales.

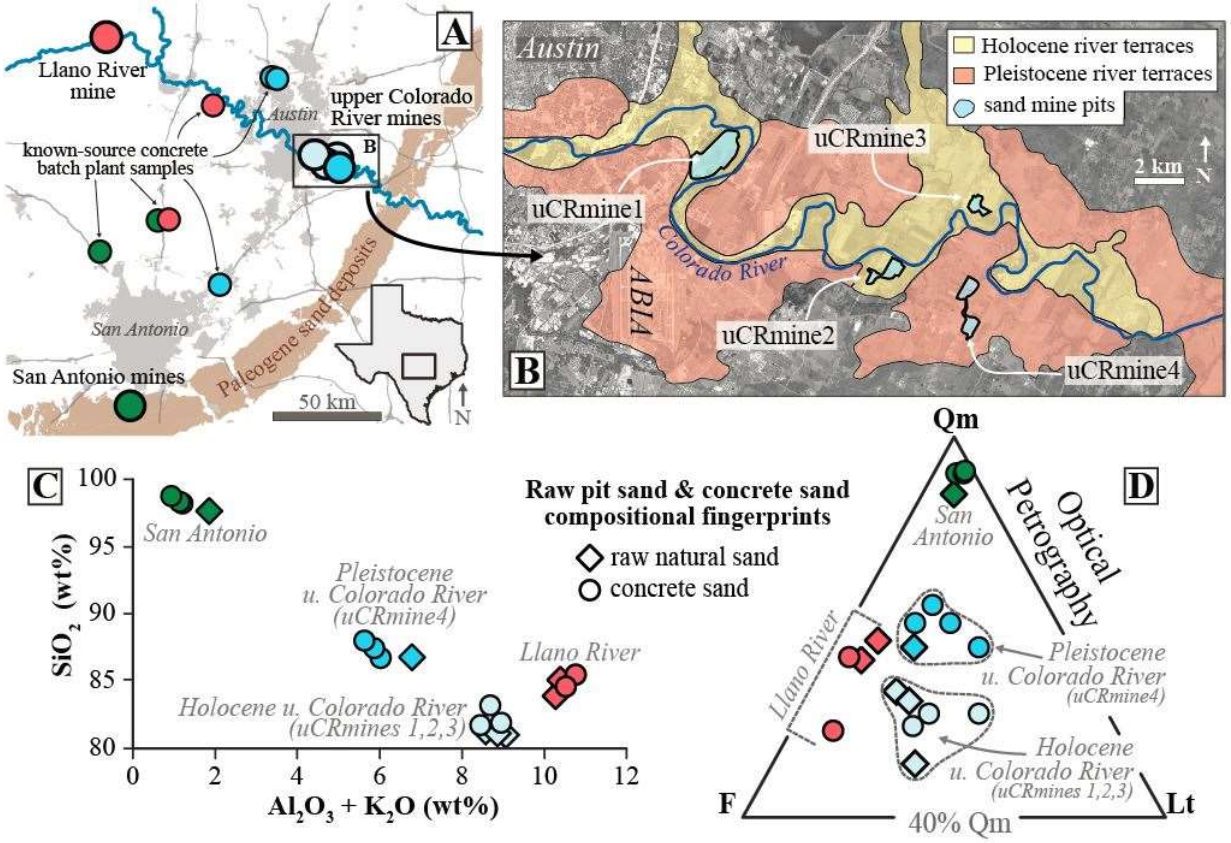

Figure 4. A) Sample location map of sand mine (n = 13) and concrete batch plant (n = 6) samples from central Texas used to test if processing affects sand compositional fingerprints. B) Inset showing the location of sand mines on the upper Colorado River south of Austin that mine from Holocene-age (24) terraces (uCRm1-3) and Pleistocene age (24) terraces (uCRm4). C) Bulk geochemistry results showing major elements, Si, Al + K content for each sample in this area. Note that the Pleistocene u. Colorado River sample cluster is comprised of five samples; two samples in the upper left plot too closely to distinguish their symbols. D) Optical petrography results for this sample set. Qm: monocrystalline quartz, F: total feldspar, Lt: total lithic fragments.

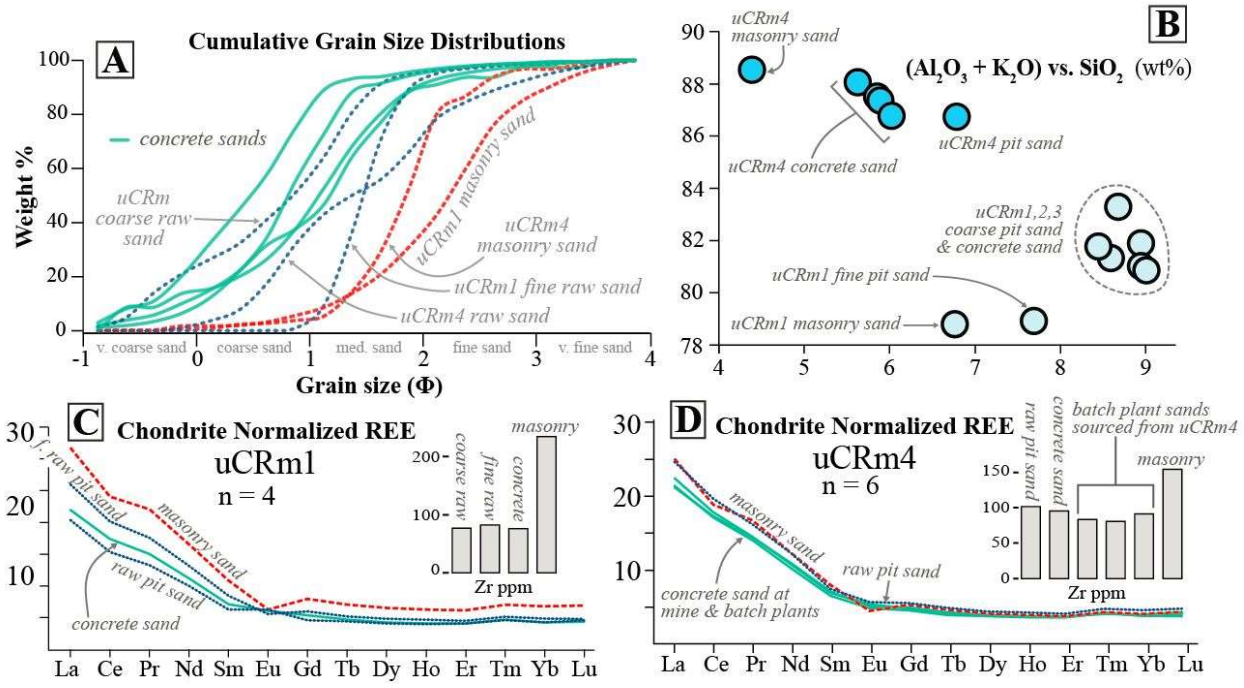

606

607 **Figure 5.** Grain size and geochemical fingerprinting results from closely spaced sand mines in Holocene
608 and Pleistocene terraces south of the City of Austin along the upper Colorado River. A) Grain size for upper
609 Colorado River mine samples displayed as Phi-scale weight percent cumulative distributions measured in
610 a settling column. Samples are colour coded by type. B) Bulk major element X-ray fluorescence analysis
611 (XRF) results for upper Colorado River mine samples. C) Chondrite normalised Rare Earth Element (REE;
612 Taylor and McClennan, 1985) signatures of sand from mining location uCRm1 which taps Holocene upper
613 Colorado River terraces. D) Chondrite normalised Rare Earth Element (REE; Taylor and McClennan, 1985)
614 signatures of sand from mining location uCRm4 which taps Pleistocene upper Colorado River terraces.
615 Note that this is the only figure that includes results for masonry sand samples.

616

617

618

619

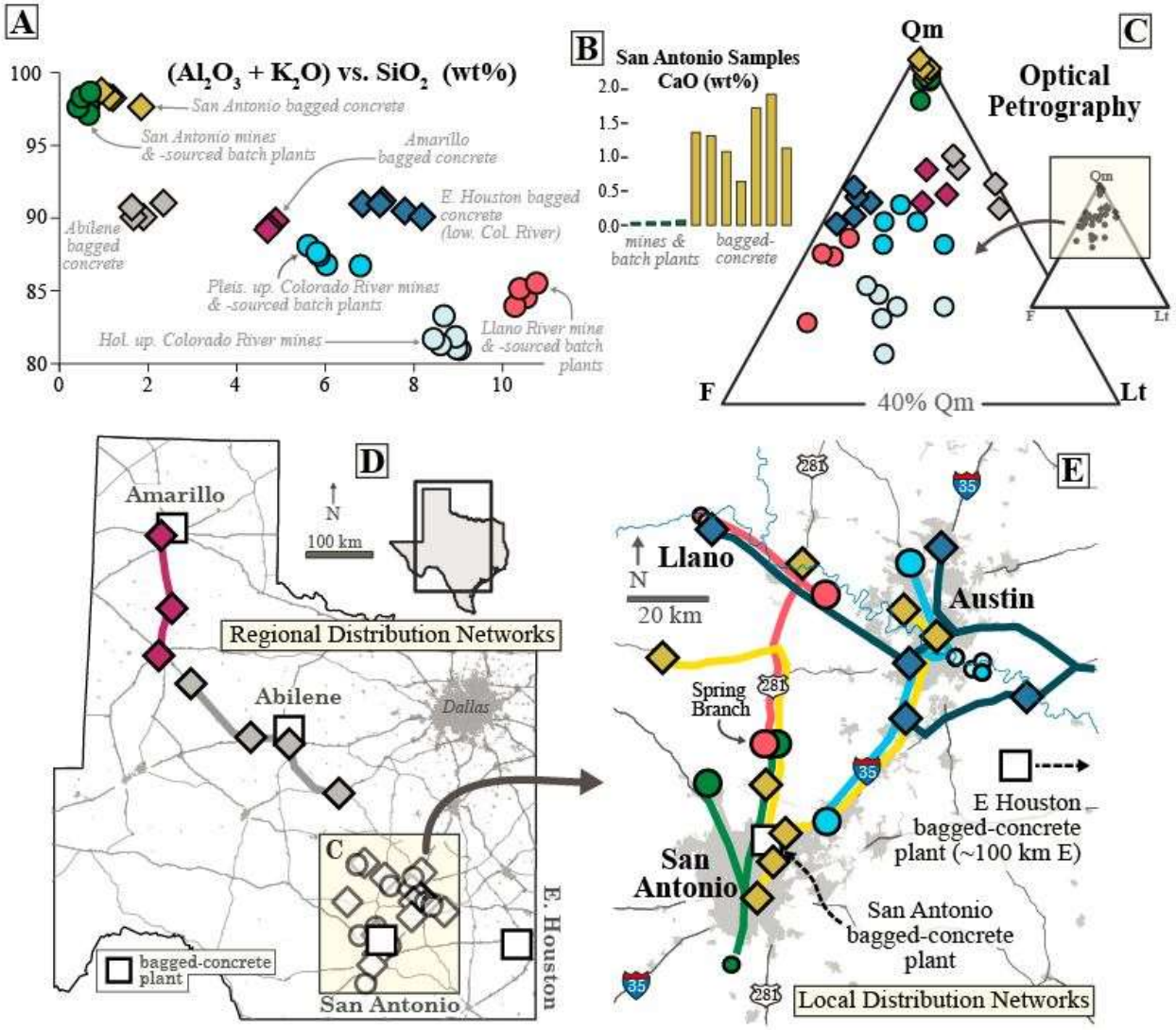

620

621 **Figure 6.** A) Bulk major element geochemistry results for sand samples from all sampled locations. B) Bar
622 graph of Ca weight % in San Antonio area samples showing artificially introduced compositional difference
623 in sand from bagged concrete. C) Optical petrography results for all samples. Note that while not as distinct
624 as bulk geochemistry results, each distribution network is distinguishable based on framework mineralogy.
625 Qm: monocrystalline quartz, F: total feldspar, Lt: total lithic fragments. D) and E) Regional supply-
626 networks traced by sand fingerprinting.

627

628

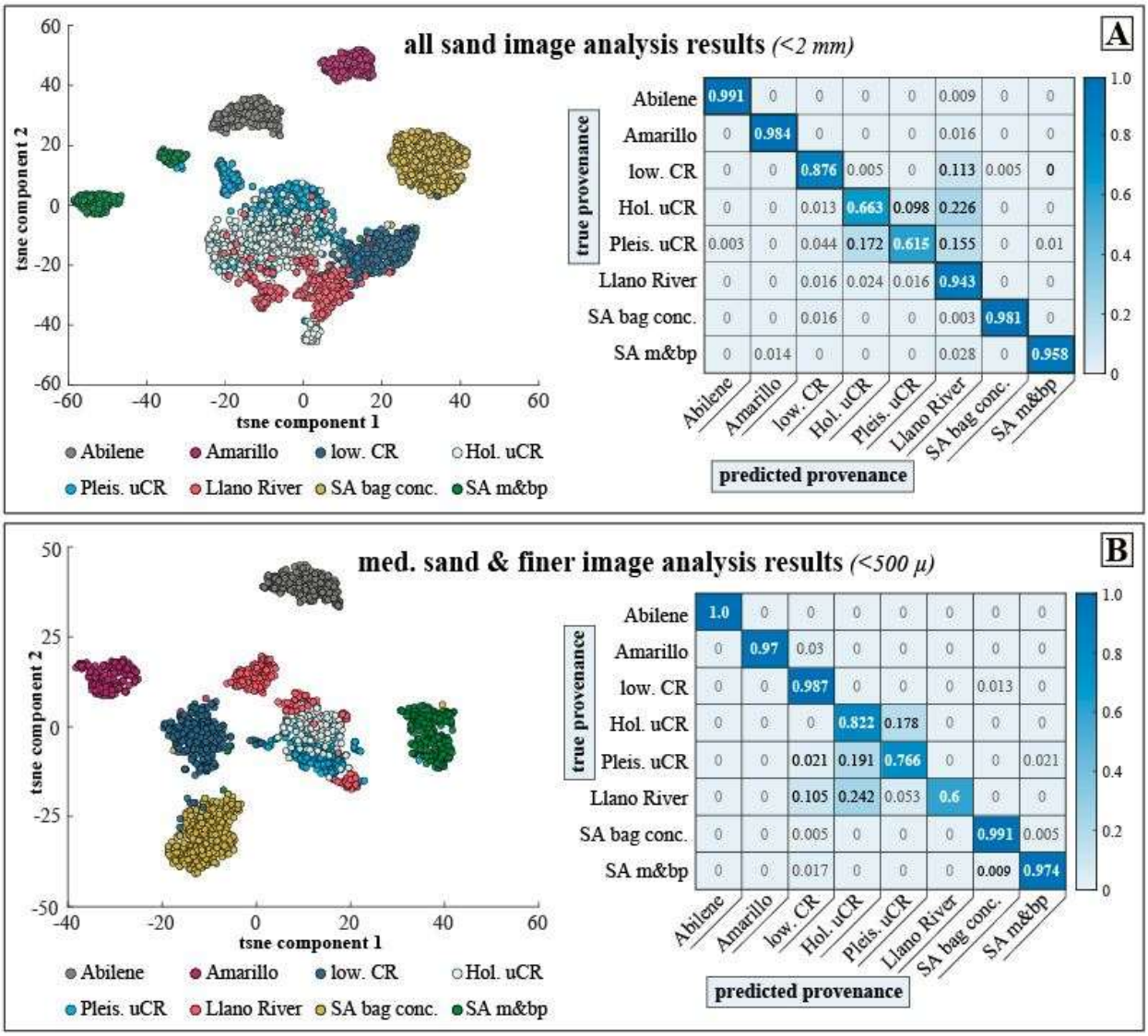

Figure 7. *sandID* image-analysis results for A) all sand samples (all material <2 mm) and B) all samples sieved at 500 microns (medium sand and finer). For both A and B: [Left] Two-dimensional, simplified representation of what the neural network "sees" as differences between each source population in images. In A) each color-coded point is a snip of a training image and distance between two points roughly correlates to degree of difference. s*andID* uses 1,024 distinct image features that are the result of repeated transformations applied as the raw image data propagates through the layers of the neural network. These features, in effect, capture what the network "thinks" of each sand sample and are the algorithmic analog of the classical provenance analysis metrics discussed in earlier sections. We employed a widely-used

638 statistical method, t-Distributed Stochastic Neighbor Embedding ("t-SNE") (Roweis and Hinton, 2002; van
639 der Maaten and Hinton, 2008), to squeeze these 1,024 features into 2-D representations that assessed
640 visually. The left-hand panels of this figure show the results of applying this procedure to each sample in
641 our dataset. [Right] Confusion matrix illustrating model success in assigning an image of sand to its correct
642 original source. low. CR: samples derived from the lower Colorado River (east Houston bagged-concrete),
643 Hol. uCR: samples derived from Holocene terraces of the upper Colorado River, Pleis. uCR: samples
644 derived from Pleistocene terraces of the upper Colorado River. SA bag conc.: San Antonio bagged concrete,
645 SA m&bp: samples from San Antonio mines and concrete batch plants.

646

647

648

649

650

651

652

653

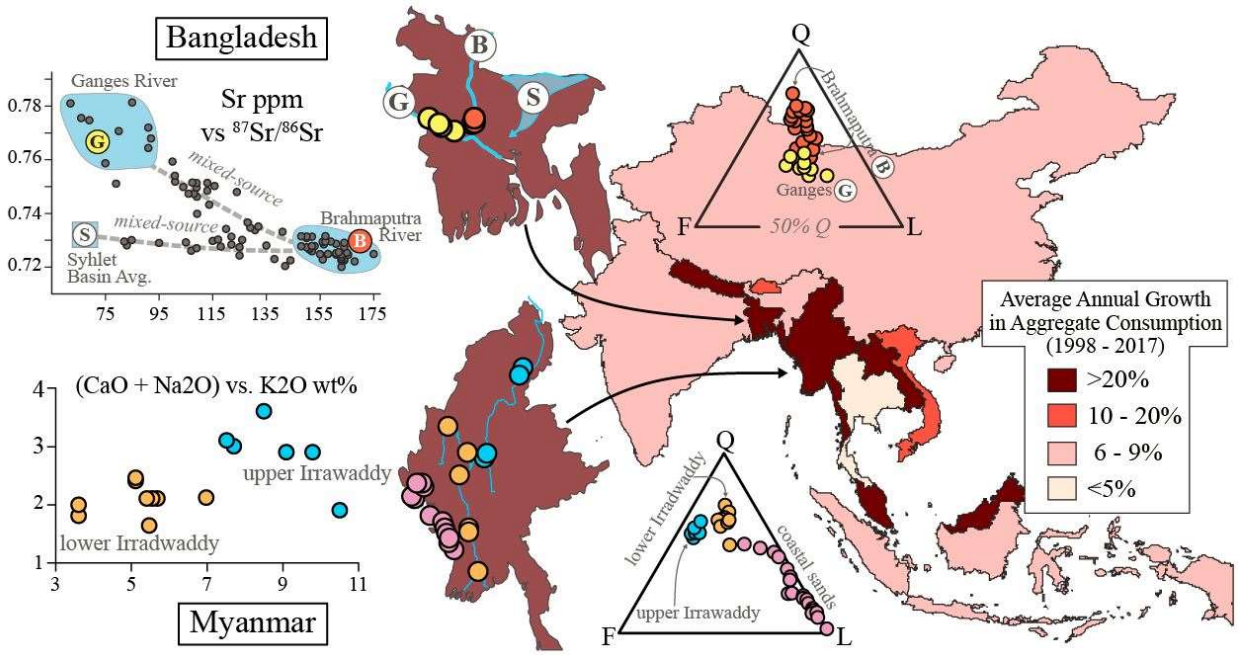

Figure 8. Example of existing compositional fingerprinting data from studies on natural sand dispersal systems illustrating potential leverage in fingerprinting construction sand-supply networks in two countries with high consumption growth rates in South and Southeast Asia; Bangladesh (32) and Myanmar (37). Aggregate consumption statistics are calculated from the UN IRP global Materials Flow database (44) and USGS Minerals Yearbook data (45).